Purity−Activity Relationships of Natural Products: The Case of Anti-TB Active Ursolic Acid

Birgit U. Jaki,[†] Scott G. Franzblau,[†] Lucas R. Chadwick,[‡,§] David C. Lankin,[‡] Fangqiu Zhang,[†,⊥] Yuehong Wang,[†] and Guido F. Pauli*[,†,‡]

Institute for Tuberculosis Research and Department of Medicinal Chemistry and Pharmacognosy, College of Pharmacy, University of Illinois at Chicago, 833 S. Wood Street, Chicago, Illinois 60612-7231

Received June 3, 2008

The present study explores the variability of biological responses from the perspective of sample purity and introduces the concept of purity−activity relationships (PARs) in natural product research. The abundant plant triterpene ursolic acid (**1**) was selected as an exemplary natural product due to the overwhelming number yet inconsistent nature of its approximate 120 reported biological activities, which include anti-TB potential. Nine different samples of ursolic acid with purity certifications were obtained, and their purity was independently assessed by means of quantitative ^{1}H NMR (qHNMR). Biological evaluation consisted of determining MICs against two strains of virulent *Mycobacterium tuberculosis* and IC_{50} values in Vero cells. *Ab initio* structure elucidation provided unequivocal structural confirmation and included an extensive ^{1}H NMR spin system analysis, determination of nearly all *J* couplings and the complete NOE pattern, and led to the revision of earlier reports. As a net result, a sigmoid PAR profile of **1** was obtained, demonstrating the inverse correlation of purity and anti-TB bioactivity. The results imply that synergistic effects of **1** and its varying impurities are the likely cause of previously reported antimycobacterial potential. Generating PARs is a powerful extension of the routinely performed quantitative correlation of structure and activity ([Q]SAR). Advanced by the use of primary analytical methods such as qHNMR, PARs enable the elucidation of cases like **1** when increasing purity voids biological activity. This underlines the potential of PARs as a tool in drug discovery and synergy research and accentuates the need to routinely combine biological testing with purity assessment.

Natural products are evolutionary shaped molecules with a profound impact on human health.[1−3] Nature's biosynthetic engine produces innumerate secondary metabolites with distinct biological properties that make them valuable as health products or as structural templates for drug discovery. Synthetic variation of structure and [quantitative] correlation of structure and activity ([Q]SAR) are widely used tools in drug discovery,[4] placing the elucidated structure and its biological potency in the center of contemplation. A common finding in the natural products literature, in particular with regard to well-established natural compounds, is that the same compound is reported to act on a myriad of targets, with very different potential, and with an inconsistent activity pattern. While the unique specificity of each individual assay and variability in the performance of the bioassays are widely accepted as potential explanations, the influence of sample purity has not been examined in a systematic manner.

Typically, when a substance is pharmacologically evaluated, the assumption is made that the sample represents a single chemical entity (SCE) or a defined mixture of known chemical entities, such as in the case of stereoisomers. Conversely, pharmacopoeias and agencies worldwide have established rigorous limits for the amounts of unacceptable impurities. According to guidelines of the International Conference on Harmonization (ICH),[5] the reported impurity thresholds in new drug applications (NDAs) are often as low as 0.05−0.03%, even for enantiomeric impurities. The relevance of minor constituents cannot be overlooked when assigning pharmacologically active principles in materials of complex origin, such as in parallel (bio)synthesis and natural products. Whenever bioactive materials require isolation from a complex matrix, they are most likely to retain residual complexity even in a refined ("pure") stage. Thus, knowledge of both known and unknown impurities becomes increasingly relevant in drug discovery and bioactive natural products.

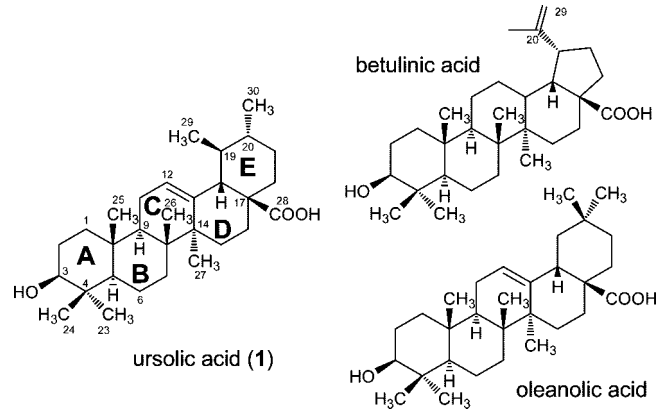

The pentacyclic plant triterpene ursolic acid (**1**, ua) exemplifies the overall situation since it appears ubiquitously in plants, has a large number of known congeneric analogues, and has a remarkable wide array of reported biological functions. A literature search using the NAPRALERT database[6] revealed 120 different bioactivities ascribed to **1** alone. Upon closer inspection, several of the reported activities are inconsistent. For example, while some report antibacterial activity[7−12] against *Staphylococcus aureus*, *Escherichia coli*, *Pseudomonas aeruginosa*, and *Bacillus subtilis*, others find **1** to be inactive against the same organisms[7,9,12−15] or even observe bacterial growth stimulation.[10] Anticytotoxic[16] and cytotoxic activity[17] have been reported against HEPG-2 cells. Furthermore, **1** has been reported as being both active and inactive in anti-inflammatory (*in vivo*, external, mouse),[18−21] cell differentiation induction (leuk-M1),[22,23] lipoxygenase-5-inhibition,[24,25] antiulcer (*in vivo*, rat),[26,27] antiyeast (*Candida albicans*),[7,11,13,15,28] and cytotoxicity (leuk P388)[29−31] assays. Due to its ubiquitous nature, **1** had been isolated from very different chemotaxonomic matrixes. This most likely resulted in very different impurity profiles of the final isolates, which were subsequently tested in the corresponding biological

* Corresponding author. Tel: (312) 355-1949. Fax: (312)-355-2693. E-mail: gfp@uic.edu.
† Institute for Tuberculosis Research.
‡ Department of Medicinal Chemistry and Pharmacognosy.
§ Current address: Cherry Instruments, 451 W. Wrightwood Ave., #306, Chicago, IL 60614.
⊥ Current address: Sanofi Pasteur Limited, 1755 Steeles Ave. West, Toronto, Ontario M2R 3T4, Canada.

10.1021/np800329j CCC: $40.75
Published on Web 09/18/2008

Table 1. ^{1}H and ^{13}C NMR Spectroscopic Data of **1**[a]

position[b]	δ_C [ppm]	δ_H [ppm]	integral	multiplicity	*J* [Hz] (coupled proton)
1a=ax	40.27	1.41[c]	1H	m[c]	2.7 (H-2ax), ~13 (H-1eq)[c]
1b=eq		0.88	1H	m[c]	2.7 (H-2ax), 3.4 (H-2eq), ~13 (H-1ax)[c]
2a=eq	28.81	1.41[c]	1H	m[c]	6.4 (H-3), 3.4 (H-1eq), ~13 (H-2 ax)[c]
2b=ax		1.42[c]	1H	m[c]	9.4 (H-3), 2.7 (H-1ax), ~13 (H-2 eq)[c]
3	80.12	2.997	1H	dd	6.4 (H-2eq), 9.4 (H-2ax)
4	40.35				
5	56.85	0.535	1H	dd	1.9 (H-6eq), 11.8 (H-6ax)
6a=ax	19.94	1.415[c]	1H	dd/m[c]	11.8 (H-5), 9.3 (H-7ax)
6b=eq		1.315[c]	1H	dd/m[c]	1.9 (H-5), 2.9 (H-7ax), 8.6 (H-7eq)
7a=ax		1.322	1H	ddd	2.9 (H-6eq), 8.6 (H-7eq), 9.3 (H-6ax)
7b=eq		1.141[c]	1H	d/m[c]	8.6 (H-7ax)
8	41.16				
9	49.14	1.320	1H	dd	5.7 (H-11eq), 11.9 (H-11ax)
10	38.56				
11a=ax	24.86	1.706	1H	ddd	3.8 (H-12), 10.8 (H-11eq), 11.9 (H-9)
11b=eq		1.729	1H	ddd	3.8 (H-12), 5.7 (H-9), 10.8 (H-11ax)
12	126.88	5.052	1H	pseudo-t	3.8 (H-11ax, H-11eq)
13	139.91				
14	43.66				
15a=ax	29.84	1.709	1H	ddd	4.1 (H-16eq), 13.6 (H-16ax), 14.1 (H-15eq)
15b=eq		0.888	1H	ddd	4.4 (H-16ax), 3.3 (H-16eq), 14.1 (H-15ax)
16a=ax	25.84	1.787	1H	ddd	4.4 (H-15eq), 13.1 (H-16eq), 13.6 (H-15ax)
16b=eq		0.901	1H	ddd	4.1 (H-15ax), 13.1 (H-16ax), 3.3 (H-15eq)
17	49.18				
18	54.35	2.014	1H	dd	1.8 (H-20), 11.4 (H-19)
19eq	40.69	1.14[c]	1H	dd/m[c]	6.6 (H_3-29), 11.4 (H-18)
20	40.48	0.83[c]	1H	dd/m[c]	1.8 (H-18), 6.2 (H_3-30)
21a=eq	32.33	1.30[c]	1H	ddd	1.3 (H-22ax), 2.9 (H-22eq), 13.0 (H-21ax)
21b=ax		1.34[c]	1H	ddd	2.2 (H-22eq), 14.0 (H-22ax), 13.0(H-21eq)
22a=eq	38.38	1.54[c]	1H	dt	2.2 (H-21ax), 2.9 (H-21eq), 12.9 (H-22ax)
22b=ax		1.51[c]	1H	dt	1.3 (H-21eq), 14.0 (H-21ax), 12.9 (H-22eq)
23	29.65	0.800	3H	s	
24	17.40	0.591	3H	s	
25	17.07	0.736	3H	s	
26	18.66	0.642	3H	s	
27	25.14	0.899	3H	s	
28	181.50				
29	22.84	0.756	3H	d	6.6 (H-19)
30	18.75	0.669	3H	d	6.2 (H-20)

[a] Solvents: $CDCl_3$ (950 μL) and DMSO (50 μL); 500/125 MHz. [b] All assignments were confirmed by gHSQC, gHMBC, and gCOSY maps; for numbering refer to structure drawing of **1**. [c] Signal pattern remains partially unclear due to severe signal overlap and higher order effects, basic multiplicities given under first-order assumptions.

assays. More generally, the high natural abundance of **1** in vascular plants raises doubts regarding the plausibility of it being a true panacea. Prompted by frequent reports[6] and the authors' own observations pointing at **1** as (a member of) the underlying anti-TB active principle, the goal of the present study was to study the influence of purity on antimycobacterial activity.

On the basis of the above, it can be hypothesized that previously investigated preparations of **1** represent a chemically heterogeneous group of samples, for which the presence of an SCE[32,33] does not necessarily apply. In order to test this hypothesis, the present study takes the following three-pronged approach to providing experimental evidence: (i) acquire a significant number of samples of **1**, isolated from various natural sources, determine their individual purity, and unambiguously confirm their structure; (ii) use state-of-the-art methods to determine their statistically significant biological activity against a target, for which significant literature reports exist; and (iii) establish PARs by correlating the level of purity with the observed biological activity. For the purpose of this study, a combination of quantitative antituberculosis and mammalian cell cytotoxicity assays was chosen. Although the innate susceptibility of mycobacterial strains to **1** was not expected to be significantly different, parallel evaluation employed two isogenic strains of *M. tuberculosis*, $H_{37}Rv$ and the GFP-carrying strain $H_{37}Rv$GFP (see Experimental Section), and two independent bioassays for the purpose of being able to recognize variability in drug susceptibility.

There are numerous reports on antimicrobial activities of **1**,[7−14,23,34,35] and triterpene aglycones have attracted particular attention as potential new leads in anti-TB drug discovery.[36−38] Accordingly, the (im)purity profile and the antimycobacterial and cytotoxic activities of nine ursolic acid samples (ua-01 to ua-09, Table 3), most of them representing compendial-quality reference materials with a certified purity of 81.00−99.57% obtained from various commercial sources, were investigated. Both impurity profiling and detailed structure elucidation were carried out by qualitative (1D and 2D NMR) and qHNMR spectroscopy, respectively.

Results and Discussion

***Ab Initio* Structure Assignment.** Despite the routine availability of high-field NMR instrumentation, such as the 500 MHz instrument used in this study or even higher field strengths, the complete analysis of the NMR spectra of triterpenes such as **1** remains a challenge in particular due to the lack of ^{1}H NMR dispersion of the signals of the tetra- and pentacyclic CH skeleton. The presence of higher order spin systems, severe signal overlap, and complex long-range coupling impede the structure elucidation process and made selective NOE experiments as well as spectra simulation necessary to solve the coupling pattern. For the present study, *ab initio* structural confirmation was performed on these molecules with the aid of ^{1}H, (APT)/^{13}C, COSY, HMQC, and HMBC spectra. The relative configuration of the stereogenic centers of the highly complex pentacyclic ring system of **1** was established by a series of selective 1D double-pulsed field gradient NOE (dpfgNOE) experiments. Although the structure of **1** has often been derived, existing reports are typically limited to carbon shifts and rather incomplete proton assignments as exemplified in ref 39.

Table 2. Purity and Bioactivity of the Nine Investigated Samples of **1** Sorted by Their Anti-TB Selectivity against Strain $H_{37}Rv$

	purity [%]			anti-TB MIC [μg/mL] (±SD)		cytotoxicity IC_{50} [μg/mL] (±SD)	anti-tb selectivity index (SI)	
sample	declared	qHNMR	Δ	$H_{37}Rv$	$H_{37}Rv$GFP	Vero cells	$H_{37}Rv$	$H_{37}Rv$GFP
ua-08	81.00	69.66	11.34	65 (±6)	30 (±2)	18 (±1)	0.28	0.61
ua-02	98.9	87.13	11.77	88 (±16)	27 (±3)	18 (±2)	0.21	0.68
ua-09	99.57	87.67	11.90	100 (±19)	31 (±5)	19 (±2)	0.19	0.62
ua-05	90.0	89.29	0.71	220 (±16)	66 (±20)	20 (±2)	0.08	0.28
ua-07	96.5	94.83	2.04	233 (±6)	n.a.	18 (±2)	0.08	n.a.
ua-04	98.6	94.65	3.81	>256[a]	64 (±24)	19 (±2)	<0.07	<0.29
ua-06	98.5	95.52	2.98	>256[a]	68 (±8)	19 (±2)	<0.07	<0.28
ua-01	98.6	97.48	1.12	>256[a]	65 (±21)	19 (±2)	<0.07	<0.29
ua-03	98.6	98.64	−0.04	>256[a]	98 (±26)	18 (±2)	<0.07	<0.19
betulinic acid				>128				
oleanolic acid				100				

[a] The highest test concentration was 256 μg/mL, which was used to create Figure 1.

Table 3. qHNMR Impurity Profiles of the Nine Investigated Samples of **1** (ua-01 to ua-09)

	impurity				impurity		
sample	#	content [%]	assignment	sample	#	content [%]	assignment
ua-01	imp 1	0.41	oleanolic acid	ua-06	imp 1	0.63	u[a]
	imp 2	1.17	u		imp 2	0.45	u
	imp 3	0.31	u		imp 3	2.16	u
	imp 4	0.13	u		imp 4	1.42	u
	imp 5	0.03	u		imp 5	0.03	u
	imp 6	0.45	u				
	imp 7	0.09	betulinic acid				
ua-02	imp 1	9.30	oleanolic acid	ua-07	imp 1	1.22	oleanolic acid
	imp 2	0.16	u		imp 2	0.40	u
	imp 3	2.06	u		imp 3	0.22	u
	imp 4	2.42	u		imp 4	0.63	betulinic acid
	imp 5	0.08	u		imp 5	1.86	u
	imp 6	0.44	u		imp 6	1.38	u
	imp 7	0.02	u		imp 7	0.16	u
	imp 8	0.30	U		imp 8	0.41	u
ua-03	imp 1	0.18	oleanolic acid	ua-08	imp 1	26.07	oleanolic acid
	imp 2	0.35	u		imp 2	0.06	u
	imp 3	0.21	u		imp 3	0.39	u
	imp 4	0.06	u		imp 4	0.63	u
	imp 5	0.45	betulinic acid		imp 5	7.18	u
	imp 6	0.13	u		imp 6	6.73	u
ua-04	imp 1	2.53	oleanolic acid	ua-09	imp 1	5.38	oleanolic acid
	imp 2	0.88	u		imp 2	1.47	u
	imp 3	0.43	u		imp 3	2.18	u
	imp 4	0.39	betulinic acid		imp 4	1.06	u
	imp 5	0.55	u		imp 5	1.84	betulinic acid
	imp 6	0.34	u		imp 6	1.08	u
	imp 7	0.77	u		imp 7	0.57	u
	imp 8	0.17	u		imp 8	0.42	u
					Imp 9	0.06	u
ua-05	imp 1	2.31	oleanolic acid				
	imp 2	0.80	u				
	imp 3	0.27	u				
	imp 4	0.15	u				
	imp 5	0.40	betulinic acid				
	imp 6	0.57	u				
	imp 7	3.71	u				
	imp 8	2.34	u				
	imp 9	0.16	u				

[a] Unassigned impurities (u) were calculated as isomers of **1**.

As summarized in Table 1 the ^{13}C NMR spectra revealed a total of 30 carbon resonances, which could be identified as seven methyl, nine methylene, and seven methine groups, along with seven quaternary carbons, one of which represents a carboxylic acid. Analysis of the COSY and selective 1D dpfgNOE spectra revealed the presence of five almost isolated ^1H spin systems, i.e., one spin system for each of the five rings A−E of the triterpene skeleton: spin system #1 of ring A (H-1ax, H-1eq, H-2eq, H-2ax, and H-3), #2 of ring B (H-5, H-6a, H-6b, H-7a, H-7b), #3 of ring C (H-9, H-11a, H-11b, H-12), #4 of ring D (H-15ax, H-15eq, H-16ax, H-16eq), and #5 of ring E (H-18, H-19eq, H_3-29, H_3-30, H-20, H-21a, H-21b, H-22ax, H-22eq). The carbon skeleton was assembled using the HMBC map. In particular, correlations from H_3-23, H-7ax, and H-7eq to C-5 established the connection of the spin systems A and B via the C-5 bridgehead; correlations from H-1ax and H-1eq to C-25, C-10, CH-9, and C-5 determined the fragment that connects the ^1H spin systems A and C. Correlations between the olefinic proton H-12 and both C-13 and CH-18 connect spin systems C and E, while E and D are connected by a fragment determined by correlations from H-22ax and H-22eq to C-28, C-17, and CH_2-16 and from H-18 to C-17, C-28, and CH_2-16. The spin systems B, C, and D are connected by a fragment, which was established by correlations from H-11ax, H-11eq, and H-9 to C-8; H-7ax and H-7eq to C-8 and C-14; and H_3-27 to C-8, C-14, and CH_2-15. Positioning of the methyl groups at C-4 was proven by HMBC correlations from H-3ax to CH_3-23 and CH_3-24, from H_3-24 to CH_3-23, and from H_3-23 to CH_3-24. The methyl groups CH_3-25 and CH_3-26 were assigned on the basis of correlations between the axial H-9 and CH_3-25 and CH_3-26. The methyl group CH_3-27 was located by correlations from H-15ax and H-15eq to CH_3-27 as well as from H_3-27 to C-8 and C-13. The vicinal CH_3 groups CH_3-29 and CH_3-30 were assigned with the aid of HMBC cross-peaks, correlating protons H-18, H-19, H-20, and H_3-30 with carbon CH_3-29, and H_3-29, H-19, H-20, H-21ax, and H-21eq with carbon CH_3-30. Finally, the carboxyl group C-28 was placed following correlations from H-22ax, H-22eq, H-16ax, and H-16eq to C-28.

Due to the severe overlap of proton signals, selective 1D NOE (selNOE) experiments and molecular modeling were essential in solving the coupling pattern of the spin systems and to derive the relative configuration. Selective excitation of the signal of H-3 and consideration of the proton distances in an energy-minimized model led to the signal assignment and the establishment of the coupling pattern of H-5 and H_3-23eq as well as the signal assignment of H-1ax. Determination of coupling constants of the C-1 and C-2 methylene protons remains partially unclear due to higher order effects and signal overlap. Selective excitation of the signal H-12 led to the unambiguous assignment of the signals of H-11ax, H-11-eq, and H-9. With the help of the selective pulse experiments it was possible to distinguish between the signals of H-11ax and H-11eq by creating a line-fitted subspectrum of spin system C, followed by spectral simulation and iteration. NOEs were detected from H-12 to two methyl groups. As only H_3-26 and H_3-30 are within a distance of 3.5 Å and below, the reported assignments of CH_3-30 and CH_3-29 need to be revised. The four signals between δ 1.709 and 1.787 could be resolved by creation of line-fitted spectra of all three signals and subtraction of the line-fitted signals of H-11ax and H-11eq, which were known from the NOE irradiation of H-12. The result was a spectrum of the signals of H-15ax and H-16eq. The signals for H-15eq and H-16eq, which both overlap

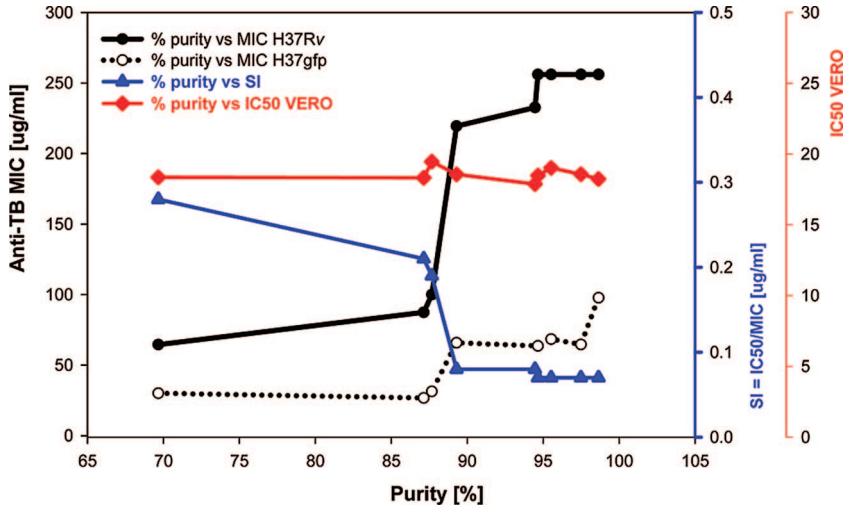

Figure 1. Purity−activity relationship (PAR) of ursolic acid. The graphic illustrates the correlation between sample *im*purity and antimycobacterial activity and proves, in turn, that there is no correlation between antimycobacterial activity and purity. This leads to the assumption that the antimycobacterial activity is not caused by the single pure compound ursolic acid, but can be related to synergic effects. Cytotoxic effects against Vero cells seem to be widely sample purity-independent. Together with the very low selectivity indices, this indicates that the cytotoxicity can be assigned to ursolic acid itself.

with methyl group signals, could, therefore, be generated by spectra simulation and optimization of the whole spin system D. SelNOE experiments with excitation of the signals of H-22ax and H-22eq, and in combination with measurements of proton distances in the force-field model, allowed the assignment, relative configuration, and the determination of coupling constants of H-21ax and H-21eq. SelNOE of H-7ax enabled the resolution of its coupling pattern and stereochemical assignment of spin system 2. Finally, excitation and spin system analysis of H-18 exhibited the dd nature of its signal, which is caused by a coupling to H-19eq, and a long-range coupling to H-20 (Table 1.).

Impurity Profiling. A combination of HPLC, routine ^{1}H NMR and, when appropriate, ^{13}C NMR represent the most frequently used methods for the purity determination of natural compounds. However, because all chromatographic methods depend on a method of detection, **1** is a problematic candidate for HPLC assays, as it lacks a UV chromophore (HPLC-DAD) and is poorly ionizable (GC- and LC-MS). While other methods such as ELSD or RI (no gradient elution!) principally allow the HPLC purity assays of **1**, UV-detection methods are still frequently used as standard methods. In order to overcome the inherent limitations of chromatography, the present study generated nonchromatographic impurity profiles of all samples by means of quantitative ^{1}H NMR (qHNMR),[33,40,41] in combination with the establishment of the above-mentioned structural dossier.

A spectral processing concept for optimizing the quantitative ^{1}H NMR spectra was developed. The best line shape (=lowest $\omega_{1/2}$) was achieved with the Lorentzian−Gaussian transformation (LG, Gaussian factor of 0.02 was better than 0.05). The best signal-to-noise (S/N) resulted from exponential multiplication (EM), the worst from LG with a Gaussian factor 0.20. For the ursolic acid samples, the optimum choice was an LG with a Gaussian factor of 0.05 and a line broadening of 0.3, which resulted in S/N between that of EM and GM. The digital resolution was increased by adding two equivalent numbers of zeros at the end of the FID data set (double zero fill). As a result, the purity of all except one of the nine ursolic acid samples was found to be notably lower than declared (Table 2), while one sample (ua-03) was slightly more pure by qHNMR than labeled ($\Delta = 0.04\%$). In three out of the nine cases the purity measured by qHNMR was found to deviate by 11−12% from the declared values.

Using qHNMR, five to nine different impurities could be determined in the samples, including oleanolic acid, which was detected in eight of the samples, and betulinic acid, which was detected in six of the samples. The identities of oleanolic and betulinic acids were verified by the following compound-specific marker signals: a doublet of a doublet split with $J = 3.4$ and 14.3 Hz at δ 2.760 (H-18) for oleanolic acid, and a doublet split with $J = 2.0$ Hz at δ 4.615 (H_2-29) for betulinic acid (Table 3).

Biological Activity. Besides providing the results of the purity evaluation, Table 2 also summarizes the antimycobacterial and cytotoxic bioactivities of the nine samples of **1**. These data led to the establishment of PARs for the anti-TB activity, the cytotoxicity, and the anti-TB selectivity of **1** (Figure 1). As expected, there were only moderate differences in the susceptibility of the two mycobacterial strains to **1** (Table 2). However, curve shape and progression demonstrate that activity and purity were *not* proportional, nor are they correlated in a linear or logarithmic fashion. Overall, an *inverse* correlation between the antimycobacterial activity and the sample purity of **1** was observed. When extrapolating the sigmoid curve in Figure 1 toward "100% purity", **1** exhibits an MIC of ≫256 and ≫100 μg/mL against $H_{37}Rv$ and $H_{37}Rv$GFP, respectively, which means that it is essentially inactive. Interestingly, at the other end of the curve, those samples with the lowest purity demonstrated the highest anti-TB activity (lowest MIC) with values as low as 27 μg/mL.

In contrast to the anti-TB properties, all samples of **1** show virtually identical cytotoxicity against Vero cells, with IC_{50} values in a very narrow range between 17.9 and 19.5 μg/mL (Table 2). Thus, while the cytotoxic activity appears to be attributable to **1** as the main component, there is no quantitative correlation of dose and response between the two. Moreover, because cytotoxicity IC_{50}'s are below anti-TB MICs throughout, the anti-TB selectivity indices (SIs) were determined to be <1 (i.e., nonselective) for both *M. tuberculosis* isogenic strains ($H_{37}Rv$ and $H_{37}Rv$GFP). Moreover, because cytotoxicity was almost identical in all nine samples, the curve representing anti-TB *selectivity* essentially represents the *inverse* of the anti-TB *activity* (Figure 1).

Quantitative Correlation of Chemistry and Biology. The above evidence supports the hypothesis that neither the antimycobacterial nor the cytotoxic activity of ursolic acid isolates is caused by **1** alone: The SCE, ursolic acid, cannot explain the sigmoid anti-TB and almost constant cytotoxicity curves in the PARs plotted in Figure 1. The latter represent a new form of quantitative correlation between chemical (purity) and biological (potency) parameters and

are additive to the definitive structural assignments that are required for establishing [Q]SARs. As a matter of fact, knowledge of PARs can be considered a prerequisite for the establishment of [Q]SARs. While PARs are *quantitative* by nature, they provide unique *qualitative* information about the SCE character[32,33,41] of a biologically active agent. Transforming this qualitative information into structural information is a separate task. In the case of ursolic acid, this turned out to be a quite challenging endeavor, reaching well beyond the scope of the current study. However, the following summarizes the numerous attempts that were made to chemically and spectroscopically characterize the "active fraction" of the impure samples of **1**.

One prerequisite for further study was the use of a loss-free separation technique, avoiding selective loss of sample constituents by irreversible adsorption, such as in silica-based LC. This made countercurrent chromatography (CCC) the method of choice.[42−44] Representing one of the least pure but most active materials, sample ua-08 was chosen as a model for further purification of the anti-TB active principle under bioassay guidance. Using high-resolution CCC methodology and applying various members of the HEMWat family of two-phase CCC solvent systems,[42,45,46] 10−50 mg aliquots of ua-08 (MIC 65 μg/mL) were separated under various HSCCC conditions (V_{tot} 120 mL, S_f ~0.55−0.75, normal and reverse phase) and fractions monitored by TLC and ^{1}H NMR. Under any of the chosen conditions and unlike analytes of typical behavior,[42,45−47] **1** always eluted as a relatively broad band, even when acid (0.1% TFA) was added to the solvent system in order to avoid the formation of pH-dependent species of **1**. At the same time, the combined fractions free of **1** showed no anti-TB activity (MIC > 128 μg/mL vs $H_{37}Rv$, mostly in four combined fractions), while MICs were between 25 and 58 μg/mL in the active part of the combined fractions that contained the bulk of **1**. The purities of all combined fractions were assessed by qHNMR and confirmed that the inactive, much more hydrophilic and lipophilic impurities had been successfully removed. The biological profiles of the obtained fractions suggest that none of the impurities had anti-TB activity (MICs > 128 μg/mL) nor were potent cytotoxic agents, while one or more must have synergistic potency, fostering a selective antimycobacterial effect. The combined qHNMR and anti-TB evaluation indicated that fractions containing **1** with ≤70% purity were more active (MICs < 50 μg/mL) than the more enriched fractions (≥85% of **1**, MICs > 70 μg/mL). This not only was in line with the observed PARs of the panel of reference materials (Figure 1) but also supported the preliminary conclusion that the residual complexity and specific composition of enriched fractions play a role in their antimycobacterial susceptibility.

Preliminary experiments showed no involvement of betulinic acid (five-membered, isopropylidene-substituted E-ring isomer of **1**) or oleanolic acid ([C-29, C-30]-20,20-dimethyl isomer of **1**) in synergistic anti-TB activity of **1**. The further specific exploration of synergy in ursolic acid samples using the isobole method, as recently demonstrated for the anti-TB ethnobotanical *Oplopanax horridus*,[48] would depend on the actual isolation of sufficient quantities of known impurities and was beyond the scope of this study.

A compelling parallel exists between the presently observed essential inactivity of **1** against mycobacteria and the report of its solubilizing properties for allelochemicals of *Calamintha ashei* and *Ceratiola ericoides*:[49] While **1** itself was found to be inactive, its presence enhanced the allelochemical potency of a number of lipophilic monoterpenes. Both the relatively weak (high critical micelle concentration [CMC]) surfactant properties and its potential to interact with membrane transport mechanisms were discussed as a potential explanation.[49] Another related interesting finding was the recent discovery of self-assembling cannabinomimetics, in which the agents, *N*-alkylamides, partition between the target and various levels of aggregates.[50] As a result, the compounds exhibit differential receptor affinity as a function of concentration. Despite the reported high CMC of **1**,[49] the formation of macromolecular aggregates and potential involvement of the impurities might offer an alternative explanation for the observed PARs of **1**. We are presently investigating whether polymorphism, a well-know source of altered pharmacology, is involved.

In summary, the anti-TB activity remained inseparable from **1** as one chemical entity and could also not be enriched in fractions that contained other chemical entities, in particular congeneric triterpenes. Taking into account the qHNMR-based PARs for anti-TB and cytotoxic activity established above, these findings support the hypothesis that one or more of the reported biological activities of ursolic acid are related to synergistic effects between ursolic acid and its common impurities, or to the impurities themselves. The observed biological effects root in nonclassical phenomena that involve complex chemical−biological interactions, such as synergy, and secondary/tertiary chemical structures, such as macromolecular and physicochemical properties that involve structural arrangements beyond the single molecule level.

A recent SAR study[51] of C-30-substituted cinnamate ester analogues of **1**, betulinic acid, and oleanolic acid concluded that the introduction of a *p*-coumarate moiety increases the anti-TB activity by 2-, 8-, and 8-fold, from MICs of 12.5, 50, and 50 μg/mL, respectively. The observed potencies and perceived potential of triterpene cinnamate esters as anti-TB drug leads in this semisynthetic study[51] are in apparent contrast to the results of the present work. However, keeping in mind that the purities of underivatized and modified products were not investigated, PARs might provide the missing link to the understanding of the underlying mechanisms.

Potential of qHNMR-Based PARs. With respect to natural products and related research involving samples of complex composition, the results of this study suggest that purity should be routinely investigated for all isolates, whenever their biological activity is deemed to be of sufficient interest as to warrant further studies. This particularly applies to drug discovery screening candidates evolving from complex matrices. Examples comprise, but are not limited to, natural products from terrestrial, marine, and microbial organisms, as well as to products of parallel and combinatorial synthesis. Since potency and selectivity are the two primary desired attributes of a hit in a screening program geared toward drug discovery, the implications of overlooking purity-related effects can be profound. The case of **1** exemplifies the importance of combining state-of-the-art structure elucidation or dereplication with the determination and report of sample purity, whenever feasible, together with the biological data. The data also underline the great potential qHNMR has in providing distinctive information about the nature and amount of impurities with virtually no additional effort.[33] qHNMR is the method of choice for purity evaluation and establishment of PARs. The latter can offer new insights when working with materials that require purification from complex matrices such as products of combinatorial or parallel (bio)synthesis and natural products, including dietary supplements.

Furthermore, the case of **1** demonstrates that the complexity of biologically active natural products extends beyond their valuable structural diversity: Whenever active principles are elucidated chemically, it is important to consider "hidden" mechanisms that might involve (apparent) SCEs and their interactions with (residually) complex natural matrices. The establishment of PARs provides a powerful tool for recognizing such "hidden" connections, in particular when employing nonchromatographic methodology such as qHNMR in the purity dimension. PAR by qHNMR carries the advantage of allowing detection of even those instances where highly complex or unknown chemical interactions are an integral part of a bioactive principle and represent concealed assets of SCE-dominated evaluation strategies. Because of their nuclear perspective[40] and ability to function well even under flawed molecular

weight assumptions,[32] qHNMR-based PARs provide an independent rationale for exploratory drug discovery efforts and can be implemented early in any workflow aimed at the discovery of bioactive principles. In addition, PARs have promise for the cross-validation of compendial reference materials.

Experimental Section

Sample Material. Ursolic acid (**1**) was obtained from nine different commercial sources (details are available upon request from the authors). All samples came with a certificate of analysis including purity assignments, which were based on HPLC assays.

Structure Elucidation and Impurity Profiling. Prior to analysis the samples were dried thoroughly over P_4O_{10} *in vacuo* to eliminate variations from residual water. Samples ranging from 4 to 11 mg were dissolved in 50 μL of DMSO (99.9% isotopic purity), and $CDCl_3$ (99.8% isotopic purity) was added to give a final volume of 1000 μL, corresponding to a filling height of 50 mm in 5 mm NMR tubes. The NMR spectra were recorded using a Bruker AMX 500 instrument. Chemical shifts (δ in ppm) were referenced to the residual $CDCl_3$ signals at δ 7.240 and 77.00, respectively, and couplings constants (J) are given in Hz. For all NMR experiments, off-line data analysis was performed using the NUTS software package, Acorn NMR Inc. The 1D digital resolution was better than 0.4 Hz, equivalent to 0.0008 ppm (32K real data points, 12 ppm spectral width), in the ^{1}H, and 0.7 Hz, equivalent to 0.006 ppm (32K real data points, 240 ppm spectral width), in the ^{13}C domain.

For (im)purity profiling, ^{1}H NMR spectra were measured with 512 scans to yield spectra suitable for a quantitative evaluation (qHNMR).[40,41] The precision of the detection of minor impurities present at ca. 1% abundance was better than 2%. All acquisition parameters were selected in agreement with quantitative NMR conditions[40,41] and without broadband ^{13}C decoupling, as this only very recently reported qHNMR methodology[33] was not available at the commencement of this study.

In the second step, a spectral processing concept for optimizing the quantitative ^{1}H NMR spectra was developed. The first objective was the determination of the optimal window function and parameters. Therefore, a study was designed to compare the $\omega_{1/2}$ (width [Hz] at half-height) of the reference signal ($CDCl_3$ singlet at 7.240 ppm) with the achieved signal-to-noise ratio when using different window functions and parameters as follows: (i) Exponential multiplication (EM), (ii) Gaussian multiplication (GM), (iii) Lorentzian−Gaussian resolution enhancement (LG) with Gaussian factor 0.05, (iiii) LG with Gaussian factor 0.20. The line-broadening value was set at 0.01−2.5 in steps of 0.1. As expected, the best line shape (=lowest $\omega_{1/2}$) was achieved with the LG (Gaussian factor 0.02 better than 0.05). The S/N resulted from the EM, the worst from LG with a Gaussian factor 0.20. For the ursolic acid samples, the optimum choice was an LG with a Gaussian factor of 0.05 and a line broadening of 0.30, which resulted in S/N between that of EM and GM. The digital resolution was increased by adding two equivalent numbers of zeros at the end of the FID data set (double zero fill). To improve integration, the baseline of the spectrum was corrected, broad water as well as other −OH and exchangeable proton signals were eliminated by repeated simulation and subtraction from the uneven baseline, and, finally, a baseline flattening was applied by nth ($n < 10$)-order polynomial correction. The doublet at δ 2.033 of the main component **1** served as a reference signal set to an arbitrary integral value of 100. 2D COSY spectra were consulted to aid in the assignment of the impurities.

Antimycobacterial Assays. *M. tuberculosis* $H_{37}Rv$ ATCC 27294 ($H_{37}Rv$) was obtained from the American Type Culture Collection (Rockville, MD). The fluorescent (GFP) strain $H_{37}Rv$-pFPCA1 ($H_{37}Rv$GFP) was constructed in the Institute for Tuberculosis Research (ITR), University of Illinois at Chicago.[52] $H_{37}Rv$ was cultured 100 mL of Middlebrook 7H9 broth (Difco, Detroit, MI) supplemented with 0.2% (v/v) glycerol (Sigma Chemical Co., Saint Louis, MO), 10% (v/v) OADC (oleic acid, albumin, dextrose, catalase; Difco), and 0.05% (v/v) Tween 80 (Sigma), a culture medium referred to as 7H9GC-T80. $H_{37}Rv$GFP was cultured identically, except that kanamycin (30ug/mL) was added. The cultures were incubated in 300 mL nephelometer flasks on a rotary shaker (New Brunswick Scientific, Edison, NJ) at 150 rpm and 37 °C until they reached an optical density of 0.4−0.5 at 550 nm. The bacteria were washed and suspended in 20 mL of phosphate-buffered saline and passed through an 8 μm pore size filter to eliminate bacterial clumps. The filtrates were aliquoted and stored at −80 °C.

Kanamycin sulfate (KM) and rifampin (RMP) were obtained from Sigma. The chemicals were solubilized according to the manufacturers' recommendations. Stock solutions were filter sterilized (0.22 μm pore size) and stored at −80 °C. The 7H12 media consisted of Middlebrook 7H9 broth supplemented with 0.1% casitone (Difco), 0.1% palmitic acid (5.6 mg/mL free acid in ethanol, Sigma), 10% albumin (50 mg/mL in water, Sigma), and 0.1% catalase (4 mg/mL in water, Sigma).

Minimum inhibitory concentrations (MIC) of the ursolic acid samples were determined using the microplate Alamar blue assay (MABA)[53] and the green fluorescent protein microplate assay (GFPMA).[52] Testing was performed in black, clear-bottomed, 96-well microplates (black view plates; Packard Instrument Company, Meriden, CT) in order to minimize background fluorescence. Initial sample dilutions were prepared in dimethyl sulfoxide, and subsequent 2-fold dilutions were performed in 0.1 mL of 7H12 media in the microplates.

The inocula were initially diluted in 7H12 media to achieve approximately 2×10^5 cfu/mL, and 0.1 mL was added to individual wells. Wells containing compounds only were used to detect autofluorescence of compounds. Additional control wells consisted of bacteria only (B) and medium only (M). Plates were incubated at 37 °C.

For the MABA assays, at day 7 of incubation of plates inoculated with $H_{37}Rv$, 20 μL of Alamar Blue solution (Trek Diagnostic Systems, Cleveland, OH) and 12.5 mL of 20% Tween 80 were added to all the wells, and plates were reincubated at 37 °C for 24 h. Fluorescence was measured in a Victor II multilabel fluorometer (Perkin-Elmer Life Sciences Inc., Boston, MA) in bottom-reading mode with excitation at 530 nm and emission at 590 nm. For the GFPMA assay, fluorescence was measured directly with excitation at 485 nm and emission at 535 nm on day 7 of incubation of plates inoculated with $H_{37}Rv$GFP. For both MABA and GFPMA, a background subtraction was performed on all wells using the mean of triplicate M wells. Percent inhibition was defined as 1 − (test well FU/mean FU of triplicate B wells) × 100. The lowest drug concentration effecting an inhibition of 90% was considered the MIC. Mean, standard deviation (SD), and coefficient of variation (CV = 100 × mean/SD) of seven replicates each were calculated for all assays.

Cytotoxicity Assay. Cytotoxic activity of compounds was determined for Vero cells (kidney, African green monkey), which had been exposed to 16−0.25 μg/mL test compounds for 72 h. The assay (n = 7) was performed using the CellTiter 96 aqueous nonradioactive cell proliferation assay (Promega Corp., Madison, WI). The IC_{50} is defined as the reciprocal dilution resulting in 50% inhibition of the Vero cells.

Chromatographic Separation. Sample ua-08, the sample with the lowest detected purity (69.66%) and the lowest MIC (64.57 μg/mL MIC $H_{37}Rv$), was subjected to further separation by means of HSCCC. A 200 mg sample, which was an ursolic acid sodium salt, was dissolved in 50 mL of $CHCl_3$ (containing 0.05 mL of TFA 0.01%), 50 mL of H_2O was added, and the two-phase solution was transferred to a separation funnel. After 15 min reaction time, the $CHCl_3$ phase (lower phase) was washed with water (upper phase) × 3. The lower phases were collected and combined. The last separation of the two phases was done overnight to get a clean two-phase system. $CHCl_3$ was evaporated to yield the free ursolic acid.

The sample was further fractionated by HSCCC with a Pharma-Tech Research Corp. instrument (CCC1000) in tail-to-head mode using various members of the HEMWat family of two-phase solvent systems.[46] The solvent system consisting of *n*-hexanes−EtOAc−MeOH−0.01% TFA in H_2O (6:4:5:5) was determined to be most suitable. For bioassay-controlled separation, a 33 mg sample of ua-08 (dissolved in equal amounts of upper and lower phase, 2 mL) was injected; 245 fractions were collected and recombined into 14 fractions, which were all subjected to mycobacterial testing ($H_{37}Rv$, MABA). The separation was monitored qualitatively by silica TLC, developed with EtOAc−*n*-hexanes (5:5) and using 2% anisaldehyde−2% H_2SO_4 in MeOH as detection reagent, as well as ^{1}H NMR of selected fractions.

Acknowledgment. The expert NMR support of Dr. R. Kleps, Research Resources Center at UIC, Chicago, and Dr. M. Westler, NMRFAM, University of Wisconsin, Madison, WI, is gratefully acknowledged. The authors are thankful to Drs. N. Farnsworth and G. Cordell of UIC, Chicago, and Dr. N. H. Fischer, Denton (TX), for fruitful discussions, and to M. L. Quinn-Beattie, NAPRALERT at UIC, Chicago, for her invaluable help with the complex literature search.

Finally, the support of W.-W. Zhao and Dr. S.-N. Chen of UIC, Chicago, is gratefully acknowledged.

References and Notes

(1) Newman, D. J.; Cragg, G. M.; Snader, K. M. *Nat. Prod. Rep.* **2000**, *17*, 215–234.
(2) Newman, D. J.; Cragg, G. M.; Snader, K. M. *J. Nat. Prod.* **2003**, *66*, 1022–1037.
(3) Newman, D. J.; Cragg, G. M. *J. Nat. Prod.* **2007**, *70*, 461–477.
(4) Lill, M. A. *Drug Discovery Today* **2007**, *12*, 1013–1017.
(5) U.S. Food and Drug Administration. Guidance for Industry. Q3A Impurities in New Drug Substances. http://www.fda.gov/cber/gdlns/ichq3a.htm#v (accessed May 31, 2008).
(6) Farnsworth, N. R. The NAPRALERT database. Available on-line through the Scientific and Technical Network (STN) of Chemical Abstracts Service, Columbus, OH, 2007.
(7) Braghiroli, L.; Mazzanti, G.; Manganaro, M.; Mascellino, M. T.; Vespertilli, T. *Phytother. Res.* **1996**, *10*, S86−S88.
(8) Mathuram, V.; Bhahmadhayalaselvam, A.; Jaffar Hussain, A.; Bhima Rao, R.; Patra, A. *J. Ind. Chem. Soc.* **1998**, *75*, 262–264.
(9) Richards, R. M.; Durham, D. G.; Liu, X. *Planta Med.* **1994**, *60*, 471–473.
(10) Takechi, M.; Tanaka, Y. *Phytochemistry* **1993**, *34*, 675–677.
(11) Panizzi, L.; Catalano, S.; Miarelli, C.; Pioni, P. l.; Campeol, E. *Phytother. Res* **2000**, *14*, 561–563.
(12) Kuroyanagi, M.; Ebihara, T.; Tsukamoto, K.; Fukushima, S.; Ishizeki, C.; Satake, M. *Screening of antibacterial constituents of crude drugs and plants*; 5th Symposium on development and application of naturally occuring drug materials; Japan, 1984.
(13) Haraguchi, H.; Kataoka, S.; Okamoto, S.; Hanafi, M.; Shibata, K. *Phytother. Res.* **1999**, *12*, 151–156.
(14) Osawa, K.; Yasuda, H.; Morita, H.; Takeya, K.; Itokawa, H. *Nat. Med.* **1997**, *51*, 365–367.
(15) Gonzales, B.; Suarez Roca, H.; Bravo, A.; Salas Auvert, R.; Avila, D. *Pharm. Biol.* **2000**, *38*, 287–290.
(16) Miura, N.; Matsumoto, Y.; Miyairi, S.; Nishiyama, S.; Naganuma, A. *Mol. Pharmacol.* **1999**, *56*, 1324–1328.
(17) Ahn, K. S.; Hahm, M. S.; Park, E. J.; Lee, H. K.; Kim, E. H. *Planta Med.* **1998**, *64*, 468–470.
(18) Manez, S.; Recio, M. C.; Giner, R. M.; Rios, J. L. *Eur. J. Pharmacol.* **1997**, *334*, 103–105.
(19) Huang, M. T.; Ho, C. T.; Wang, Z. Y.; Ferraro, T.; Lou, Y. R.; Stauber, K.; Ma, W.; Georgiadis, C.; Laskin, J. D.; Conney, A. H. *Cancer Res.* **1994**, *54*, 701–708.
(20) Huguet, A. I.; Del Carmen Recio, M.; Manez, S.; Giner, R. M.; Rios, J. L. *Eur. J. Pharmacol.* **2000**, *410*, 69–81.
(21) Yasukawa, K.; Takido, M.; Takeuchi, M.; Nakagawa, S. *Chem. Pharm. Bull.* **1989**, *37*, 1071–1073.
(22) Umehara, K.; Takagi, R.; Kuroyanagi, M.; Ueno, A.; Taki, T.; Chen, Y. J. *Chem. Pharm. Bull.* **1992**, *40*, 401–405.
(23) Liu, J. *J. Ethnopharmacol.* **1995**, *49*, 57–68.
(24) Ali, R. M.; Houghton, P. J. *Planta Med.* **1999**, *65*, 455–457.
(25) Simon, A.; Najid, A.; Chulia, A. J.; Delage, C.; Rigaud, M. *Biochim. Biophys. Acta* **1992**, *1125*, 68–72.
(26) Ma, X. H.; Zhao, Y. C.; Yin, L.; Xu, R. L.; Han, D. W.; Wang, M. S. *Yao Hsueh Hsue Pao* **1986**, *21*, 332–335.
(27) Okuyama, E.; Yamazaki, M.; Ishii, Y. *Shoyakugaku Zasshi* **1983**, *37*, 52–55.
(28) Kim, D. W.; Bang, K. H.; Rhee, Y. H.; Lee, K. T.; Park, H. J. *Arch. Pharm. Res.* **1998**, *21*, 688–691.
(29) Lee, K. H.; Lin, Y. M.; Wu, T. S.; Zhang, D. C.; Yamagishi, T.; Hayashi, T.; Hall, I. H.; Chang, J. j.; Wu, R. Y.; Yang, T. H. *Planta Med* **1988**, *54*, 308–311.
(30) Han, G. Q.; Che, C. T.; Fong, H. H. S.; Farnsworth, N. R.; Phoebe, C. H. J. *Fitoterapia* **1988**, *59*, 242–244.
(31) Numata, A.; Takahashi, C.; Miyamoto, T.; Yoneda, M.; Yang, P. *Chem. Pharm. Bull.* **1990**, *38*, 942–944.
(32) Pauli, G. F.; Jaki, B. U.; Lankin, D. C.; Walter, J. A.; Burton, I. W. *Quantitative NMR (qNMR) of Bioactive Natural Products in Bioactive Natural Products: Detection, Isolation and Structural Determination*, 2nd ed.; Colegate, S. M., Molyneux, R. J., Eds.; Taylor & Francis: New York, 2008.
(33) Pauli, G. F.; Jaki, B.; Lankin, D. *J. Nat. Prod.* **2007**, *70*, 589–595.
(34) Schühly, W.; Heilmann, J.; Calis, I.; Sticher, O. *Planta Med.* **1999**, *65*, 740–743.
(35) Isobe, T.; Noda, Y.; Ohsaki, A.; Sakanaka, S.; Kim, M.; Taniguchi, M. *Yakugaku Zasshi* **1989**, *109*, 175–178.
(36) Cantrell, C. L.; Franzblau, S. G.; Fischer, N. H. *Planta Med.* **2001**, *67*, 685–694.
(37) Copp, B. R.; Pearce, A. N. *Nat. Prod. Rep.* **2007**, *24*, 278–297.
(38) Newton, S. M.; Lau, C.; Wright, C. W. *Phytother. Res.* **2000**, *14*, 303–322.
(39) Weiss, R.; Seebacher, W. *Magn. Reson. Chem.* **2002**, *40*, 455–457.
(40) Pauli, G. F. *Phytochem. Anal.* **2001**, *12*, 28–42.
(41) Pauli, G. F.; Jaki, B.; Lankin, D. *J. Nat. Prod.* **2005**, *68*, 133–149.
(42) Berthod, A.; Friesen, J. B.; Inui, T.; Pauli, G. F. *Anal. Chem.* **2007**, *79*, 3371–3382.
(43) Ito, Y. *J. Chromatogr. A* **2005**, *1065*, 145–168.
(44) Berthod, A. *Countercurrent Chromatography: The Support-free Liquid Stationary Phase*, 1st ed.; Elsevier: Amsterdam, 2002; Vol. 38.
(45) Friesen, J. B.; Pauli, G. F. *J. Agric. Food Chem.* **2008**, *56*, 19–28.
(46) Friesen, J. B.; Pauli, G. F. *J. Liq. Chromatogr. Relat. Technol.* **2005**, *28*, 2877–2808.
(47) Friesen, J. B.; Pauli, G. F. *J. Chromatogr. A* **2007**, *1151*, 51–59.
(48) Inui, T.; Wang, Y.; Deng, S.; Smith, D.; Franzblau, S.; Pauli, G. F. *J. Chromatogr. A* **2007**, *1151*, 211–215.
(49) Tanrisever, N. *Plant Germination and Growth Inhibitors from Ceratiola ericoides and Calamintha ashei*; Louisiana State University: Baton Rouge, 1986.
(50) Raduner, S.; Bisson, W.; Abagyan, R.; Altmann, K. H.; Gertsch, J. *J. Nat. Prod.* **2007**, *70*, 1010–1015.
(51) Tanachatchairatana, T.; Bremner, J. B.; Chokchaisiri, R.; Suksamrarn, A. *Chem. Pharm. Bull.* **2008**, *56*, 194–198.
(52) Changsen, C.; Franzblau, S. G.; Palittapongarnpim, P. *Antimicrob. Agents Chemother.* **2003**, *47*, 3682–3687.
(53) Collins, L.; Franzblau, S. *Antimicrob. Agents Chemother.* **1997**, *41*, 1004–1009.

NP800329J